Thermal Dimerization of 1-Substituted-3,4-Dimethylphospholes within the Coordination Sphere of Platinum(II)

William L. Wilson,† Jeffrey A. Rahn,† Nathaniel W. Alcock,‡ Jean Fischer,§ John H. Frederick,† and John H. Nelson*,†

Departments of Chemistry, University of Nevada, Reno, Nevada 89557, University of Warwick, Coventry CV47AL, England, and Laboratoire de Cristallochimie et de Chimie Structurale (URA 424-CNRS), Université Louis Pasteur, 67070 Strasbourg, Cedex, France

Received July 21, 1993®

The thermolyses of dihalobis(1-substituted-3,4-dimethylphosphole)platinum(II) complexes were investigated in 1,1,2,2-tetrachloroethane solutions at 145 °C and in the crystalline state at 140 °C. Three types of species were formed: (1) [4 + 2] cycloaddition products, (2) [2 + 2] cycloaddition products, and (3) compounds that result from 1,5-hydrogen migration from a methyl group on one phosphole to the β-carbon of an adjacent phosphole (*exo*-methylene). Kinetic studies suggest that the reaction mechanisms are the same in both the solid and solution states and that the products emanate from a common biradical intermediate. The solid-state reactions show a high degree of topotacticity with the *exo*-methylene products being ultimately formed in quantitative yields after about 24 h at 140 °C. Though the reactions in solution are slightly faster than those in the solid state, the latter are more selective. The relative reaction rates and product distributions are functions of both the phosphorus substituent and the halide. A representative example of each complex type has been characterized by single-crystal X-ray crystallography.

Introduction

During the investigation of halide and phosphine redistribution reactions of dihalobis(1-substituted-3,4-dimethylphosphole)platinum(II) complexes it was observed that in certain reactions a dimerization of the 3,4-dimethylphosphole occurs.[1,2] This was also observed in the study of bis(1-substituted-3,4-dimethylphosphole)platinum tribromostannate complexes.[3] Transition metals activate both vinyl phosphines and phospholes toward [4 + 2] cycloaddition reactions.[1,2,4,5] Since the $(phosphole)_2PtX_2$ complexes had been made[6] and were thought to be stable in solution, it was originally proposed that these dimerizations were brought about by an induced electronic asymmetry in either the $(phosphole)_2PtXX'$ species (**B** and **C**) or in the dimeric species **A** (Scheme 1). In **A** the vinyl moieties of the axial phosphole would be differently polarized from the phosphole in the basal part of the dimer. In **B** and **C** each phosphole is trans to a different trans influencer (i.e. for **B** a halide and a trihalostannate and for **C** two different halides) producing differing polarization. These charge asymmetries would be expected to provide a directing influence for the initial carbon–carbon bond formation. As shown in this paper, though, this proved not to be the case.

Experimental Section

A. Reagents and Physical Measurements. All the $(phosphole)_2PtX_2$ complexes were prepared as previously described[6] except for dichlorobis(1-phenyl-3,4-dimethylphosphole)platinum(II), $(DMPP)_2PtCl_2$, whose preparation is described below. Elemental analyses were performed by Galbraith Laboratories, Knoxville, TN. $^{31}P\{^1H\}$ NMR spectra were recorded at 40.26 MHz on a JEOL FX-100 spectrometer in the FT mode or at 121.65 MHz on a GE GN-300 spectrometer. ^1H, $^1H\{^{31}P\}$, and $^{13}C\{^1H\}$ NMR spectra were recorded at 300, 300, and 75 MHz, respectively, on a GE GN-300 spectrometer. Two-dimensional spectra were obtained as previously described.[7] Proton and carbon chemical shifts are relative to internal Me_4Si, while phosphorus chemical shifts are relative to external 85% H_3PO_4 with a positive value being down field of the respective reference.

Scheme 1

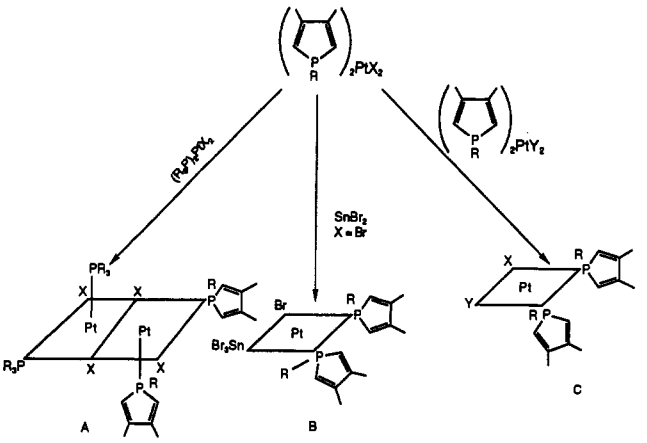

B. Improved Preparation of Dichlorobis(1-phenyl-3,4-dimethylphosphole)platinum(II), $(DMPP)_2PtCl_2$. To a vigorously stirred emulsion of 5.00 g (0.012 mol) of potassium tetrachloroplatinate(II) dissolved in 150 mL of distilled water and 150 mL of dichloromethane was added, under N_2 via syringe, 4.40 mL (0.0233 mol) of 1-phenyl-3,4-dimethylphosphole. The aqueous phase became paler and the organic phase became yellow. The reaction mixture was stirred overnight whereupon the aqueous phase became very pale red and the organic phase orange-yellow. The organic phase was removed by separatory funnel, dried with anhydrous magnesium sulfate, and gravity filtered into a 500-mL round-bottom flask. The solvent was removed by rotary evaporation using a water bath. The temperature of the water bath was gradually raised from room temperature

* Author to whom correspondence should be addressed.
† University of Nevada.
‡ University of Warwick.
§ Université Louis Pasteur.
® Abstract published in *Advance ACS Abstracts,* December 1, 1993.

(1) Rahn, J. A.; Holt, M. S.; Gray, G. A.; Alcock, N. W.; Nelson, J. H. *Inorg. Chem.* **1989**, *28*, 217.
(2) Rahn, J. A.; Holt, M. S.; Nelson, J. H. *Polyhedron* **1989**, *8*, 897.
(3) Wilson, W. L.; Nelson, J. H.; Rahn, J. A.; Alcock, N. W.; Fischer, J. *J. Phosphorus, Sulfur Silicon* **1993**, *77*, 29.
(4) Affandi, S.; Nelson, J. H.; Fischer, J. *Inorg. Chem.* **1989**, *28*, 4536.
(5) Vac, R.; Nelson, J. H.; Milosavljevic', E. B.; Solujic, L.; Fischer, J. *Inorg. Chem.* **1989**, *28*, 4132.
(6) MacDougall, J. J.; Nelson, J. H.; Mathey, F. *Inorg. Chem.* **1982**, *21*, 2145.
(7) Nelson, J. H.; Affandi, S.; Gray, G. A.; Alyea, E. C. *Magn. Reson. Chem.* **1987**, *25*, 774.

0020-1669/94/1333-0109$04.50/0

Table 1. Product Distribution in the Thermolyses of (1-substituted-3,4-dimethylphosphole)$_2$PtX$_2$ in 1,1,2,2-Tetrachloroethane at 145 °C after 18 h[a]

substituent	X	D:[4 + 2]	E:[2 + 2]	F:[*exo*-methylene]
Me	Cl	69	23	8
Ph	Cl	57	23	20
Bu^t	Cl		81	19
Bu^n	Br	21	46	33
Bzl	Br	58	14	28
Bu^t	Br		66	34

[a] Expressed as percent.

to boiling over a period of about 1 h. The removal of the dichloromethane in this manner resulted in a foamy glass. The flask was removed hot from the rotary evaporator and just enough benzene was added to the hot flask to dissolve the foamy glass. The flask was allowed to cool undisturbed whereupon 1–5-mm crystals of dichlorobis(1-phenyl-3,4-dimethylphosphole)platinum(II) slowly grew from the solution. These were isolated by gravity filtration, rinsed with diethyl ether, and allowed to air dry (yield: 5.03 g, 75.0%). Another crop of crystals could be obtained by removal of the solvent from the mother liquor redissolving in dichloromethane and repeating the process (overall yield: 6.90 g, 91.9%). The compound isolated in this manner is identical to that prepared previously[6] but with no impurities derived from the dimerization of the ligand in the recrystallization process or trace quantities for excess phosphole. Anal. Calcd for $C_{24}H_{26}Cl_2P_2Pt$: C, 44.89; H, 4.05; Cl, 11.04. Found: C, 44.78; H, 4.16; Cl, 11.00.

C. Thermolyses of Dihalobis(1-substituted-3,4-dimethylphosphole)-platinum(II) Complexes. Approximately 0.20 g of the various complexes were dissolved in 50 mL of tetrachloroethane in a 100-mL round-bottom flask fitted with a reflux condenser and N_2 outlet. The solutions were brought to reflux and refluxed for 18 h. $^{31}P\{^1H\}$ NMR spectra of the reaction mixtures were used to determine the relative amounts of the various products: **D**, the [4 + 2] cycloaddition product, **E**, the [2 + 2] cycloaddition product, and **F**, the *exo*-methylene product (see text). The results are given in Table 1.

D. Preparation of Compounds 1 and 2. A solution containing 0.50 g of dibromobis(1-*tert*-butyl-3,4-dimethylphosphole)platinum(II), in 50 mL of tetrachloroethane was heated at reflux for 18 h, resulting in a mixture of compounds **1** and **2**. The solvent was removed by rotary evaporation. The resulting mixture was recrystallized repeatedly by slow diffusion of diethyl ether into a nitromethane solution yielding 0.10 g of **1**. The soluble fractions were combined and recrystallized by the same method to give crystals of **2**, 0.10 g. Anal. Calcd for $C_{20}H_{34}Br_2P_2Pt$: C, 34.76; H, 4.92; Br, 23.12. Found for **1**: C, 34.68; H, 4.86; Br, 23.21. Found for **2**: C, 34.71; H, 4.90; Br, 22.97. ^1H NMR ($CDCl_3$, 300 MHz) for **1**: δ 1.36 (D, $|^3J(PH) + {}^5J(PH)|$ = 16.50 Hz, 18H, $C(CH_3)_3$), 1.49 (s, 6H, CH_3, 6, 11), 1.83 (T, $|^4J(PH) + {}^6J(PH)|$ = 3.00 Hz, $^5J(PtH)$ = 13.22 Hz, 6H, CH_3, 5, 12), 2.90 (AA'XX', $^3J(HH)$ = 10.82 Hz, $^2J(PH)$ = 13.44 Hz, $^3J(PH)$ = 3.39 Hz, $^2J(PP)$ = 4.51 Hz, $^3J(PtH)$ = 13.82 Hz, 2H, HC_4C_7), 5.99 (apparent dd, $^2J(PH)$ = 27.95 Hz, $^4J(PH)$ = 1.20 Hz, 2H, HC_1C_{10}). $^{13}C\{^1H\}$ NMR ($CDCl_3$, 75 MHz) for **1**: δ 17.74 (T, $|^3J(PC) + {}^5J(PC)|$ = 12.62 Hz, $C_{6,11}$), 21.72 (s, $^4J(PtC)$ = 23.28 Hz, $C_{5,12}$), 28.28 (s, $^3J(PtC)$ = 14.06 Hz, $C(CH_3)_3$), 35.00 (D, $|^1J(PC) + {}^3J(PC)|$ = 28.64 Hz, $^2J(PtC)$ = 29.02 Hz, $C(CH_3)_3$), 44.15 (5L, $^1J(PC)$ = 33.60 Hz, $^3J(PC)$ = 6.97 Hz, $^2J(PP)$ = 4.51 Hz, $^2J(PtC)$ = 108.53 Hz, $C_{4,7}$), 65.60 (T, $|^2J(PC) + {}^4J(PC)|$ = 31.87 Hz, $^3J(PtC)$ = 25.70 Hz, $C_{3,8}$), 122.11 (D, $|^1J(PC) + {}^3J(PC)|$ = 76.69 Hz, $^2J(PtC)$ = 22.60 Hz, $C_{1,10}$), 157.76 (s, $C_{2,9}$).

E. Solid-State Thermolysis of Dichlorobis(1-phenyl-3,4-dimethylphosphole)platinum(II). Dichlorobis(1-phenyl-3,4-dimethylphosphole)platinum(II), 0.200 g, was sealed in a break-seal ampule under air and heated in a drying oven at 140 °C for 30 h, yielding 0.200 g (100%) of the *exo*-methylene compound **3**. Anal. Calcd for $C_{24}H_{26}Cl_2P_2Pt$: C, 44.89; H, 4.05; Cl, 11.04. Found: C, 44.74, H, 4.16; Cl, 11.00. ^1H NMR (CD_3NO_2, 300 MHz): δ 1.35 (d, $^3J(H_4CH_3)$ = 7.51 Hz, 3H, CH_3(b)), 2.04 (apparent dt, $^4J(P_2CH_3)$ = 2.1 Hz, $^4J(H_5CH_3)$ = $^4J(H_4CH_3)$ = 1.0 Hz, $^4J(PtH)$ = 12 Hz, 3H, CH_3(a)), 2.14 (apparent qt, $^3J(H_3H_4)$ = $^3J(PH)$ = 7.6 Hz, $^3J(H_4CH_3)$ = 1.0 Hz, 1H, H_4), 2.32 (apparent t, $^4J(H_1CH_3)$ = $^4J(PH)$ = 1.5 Hz, $^5J(PtH)$ = 3.0 Hz, 3H, CH_3(c)), 2.96 (apparent dtd, $^3J(P_1H_3)$ = 35.87 Hz, $^3J(H_2H_3)$ = $^2J(P_2H_3)$ = 10.68 Hz, $^3J(H_3H_4)$ = 7.60 Hz, 1H, H_3), 3.53 (dd, $^2J(H_2H_3)$ = 10.68 Hz, $^2J(P_1H_2)$ = 6.1 Hz, 1H, H_2), 5.51 (s, 1H, H_6 or H_7), 5.80 (s, 1H, H_7 or H_6), 6.20 (d, $^2J(P_2H_5)$ = 30.0 Hz, 1H, H_5), 6.50 (d, $^2J(P_2H_1)$ = 30.0 Hz, 1H, H_1), 7.2–7.6 (m, 10H, Ph). $^{13}C\{^1H\}$ NMR (CD_3NO_2, 75 MHz): δ 14.21 (d, $^3J(PC)$ = 14.21 Hz, CH_3(c)), 18.24 (d, $^3J(PC)$ = 16.32 Hz, CH_3(a)), 21.30 (d, $^3J(PC)$ = 6.88 Hz, CH_3(b)), 45.75 (d, $^2J(PC)$ = 9.14 Hz, C_2), 48.85 (dd, $^1J(PC)$ = 45.88 Hz, $^2J(PC)$ = 13.23 Hz, $^2J(PtC)$ = 121 Hz, C_7), 55.04 (dd, $^1J(PC)$ = 42.32 Hz, $^2J(PC)$ = 10.20 Hz, $^2J(PtC)$ = 121 Hz, C_1), 113.58 (d, $^1J(PC)$ = 66.58 Hz, C_4), 117.59 (d, $^3J(PC)$ = 9.45 Hz, $^4J(PtC)$ = 23 Hz, C_{12}), 119.91 (d, $^1J(PC)$ = 55.85 Hz, $^2J(PtC)$ = 30 Hz, C_{10}), 128.80 (d, $^3J(PC)$ = 15 Hz, C_m), 129.00 (d, $^3J(PC)$ = 15 Hz, C_m), 132.50 (d, $^2J(PC)$ = 15.0 Hz, C_o), 132.7 (d, $^2J(PC)$ = 15.0 Hz, (C_o), 133.3 (s, C_p), 133.5 (s, C_p), 146.3 (dd, $^2J(PC)$ = 12.09 Hz, $^3J(PC)$ = 8.24 Hz, C_8), 160.18 (d, $^2J(PC)$ = 7.48 Hz, C_3), 165.38 (d, $^2J(PC)$ = 14.74 Hz, C_9).

F. Synthesis of Compound 4. A solution containing 0.134 g (0.2 mmol) of dichlorobis(1-phenyl-3,4-dimethylphosphole)platinum(II), $(DMPP)_2PtCl_2$, and 0.172 g (0.21 mmol) $(DMPP)_2PtI_2$ in 50 mL of $CHCl_3$ was heated at reflux for 2 weeks. The solvent was removed on a rotary evaporator and the residue was dissolved in approximately 7 mL of $CDCl_3$ and left at ambient temperature for an additional 4 weeks. The light yellow precipitate that formed was isolated by filtration and dissolved in 100 mL of CH_2Cl_2. To this solution was added a solution containing 1 g of NaI in 20 mL of 80% CH_3OH/H_2O and this mixture was stirred magnetically for 24 h. The solvent was removed by rotary evaporation, and the product was extracted with dry CH_2Cl_2. Addition of 95% ethanol induced crystallization of yellow needles which were isolated by filtration and vacuum-dried overnight: yield 0.089 g (25.9%); mp 284–286 °C. Anal. Calcd for $C_{24}H_{26}I_2P_2Pt$: C, 34.93; H, 3.18. Found: C, 35.05; H, 3.13. ^1H NMR ($CDCl_3$, 300 MHz): δ 1.16 (s, 3H, CH_3(b)), 1.50 (s, 3H, CH_3(d)), 1.61 (s, 3H, CH_3(c)), 2.01 (dd, $^4J(PH)$ = 2.4 Hz, $^4J(HH)$ = 1.4 Hz, 3H, CH_3(a)), 2.48 (apparent dt, $^3J(P'H)$ = 44.2 Hz, $^2J(PH)$ = $^3J(H_1H_2)$ = 3.4 Hz, 1H, H_2), 3.22 (d, $^2J(PH)$ = 1.9 Hz, 1H, H_4), 3.69 (apparent dt, $^3J(PH)$ = 44.1 Hz, $^2J(PH)$ = $^3J(H_1H_2)$ = 3.4 Hz, 1H, H_1), 6.25 (dq, $^2J(PH)$ = 30.2 Hz, $^4J(HH)$ = 1.4 Hz, 1H, H_3), 7.2–7.6 (m, 10H, Ph). $^{31}P\{^1H\}$ NMR ($CDCl_3$, 40.26 MHz): δ 40.6 (d, $^2J(PP)$ = 12 Hz, $^1J(PtP)$ = 2893 Hz, P), 112.5 (d, $^2J(PP)$ = 12 Hz, $^1J(PtP')$ = 2993 Hz, P').

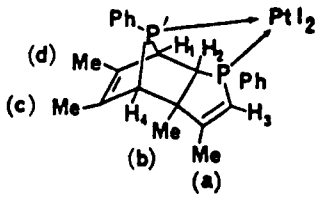

4

F. Solution Kinetics for the Thermolysis of Dichlorobis(1-phenyl-3,4-dimethylphosphole)platinum(II) in Tetrachloroethane at 145 °C. Dichlorobis(1-phenyl-3,4-dimethylphosphole)platinum(II), 10.00 g, was added to 125 mL of gently refluxing 1,1,2,2-tetrachloroethane in a 250-mL, 2-neck, round-bottom flask fitted with a rubber septum and a reflux condenser with a N_2 outlet. Samples were removed periodically and their contents determined by $^{31}P\{^1H\}$ NMR spectroscopy at 121.65 MHz.

G. Solid-State Kinetics for the Thermolysis of Dichlorobis(1-phenyl-3,4-dimethylphosphole)platinum(II) at 140 °C. The 100-mg samples of dichlorobis(1-phenyl-3,4-dimethylphosphole)platinum(II) were sealed in break-seal ampules under nitrogen and placed in a drying oven maintained at 140 °C. Samples were removed periodically and dissolved in $CDCl_3$, and the contents were analyzed by $^{31}P\{^1H\}$ NMR spectroscopy at 121.65 MHz.

H. Numerical Simulations of Unimolecular Multiple Isomerization Reaction Kinetics. Simulations of the unimolecular reaction kinetics were generated by numerically integrating the first-order differential rate equations (eqs 1–5) (*vide infra*). The integration algorithm used was a fourth-order multistep Gear algorithm with variable step size used to maintain a normalized error between 1.0×10^{-6} and 1.0×10^{-8}. An average time step of 0.5 h was found to be sufficient to maintain this accuracy for the present rate constants. Back-integration of the final product concentrations reproduced the initial conditions to eight decimal places.

I. X-ray Data Collection and Processing. Pale yellow crystals of **1** and **2** were obtained from $CH_3NO_2/(C_2H_5)_2O$ and yellow crystals of **4** were obtained from CH_2Cl_2/95% C_2H_5OH. Crystal data and details of data collection are given in Table 2. For **2**, single crystals were cut from a cluster of crystals. Systematic searches in reciprocal space with an Enraf-Nonius CAD4-F diffractometer showed that crystals of **1** and **2**

Table 2. Crystallographic Data for **1**, **2**, and **4**

chem formula	$C_{20}H_{34}Br_2P_2Pt$	$C_{20}H_{34}Br_2P_2Pt$	$C_{24}H_{26}I_2P_2Pt{\cdot}CHCl_3$
fw	691.35	691.35	825.3 + 119.4
cryst syst	orthorhombic	monoclinic	monoclinic
a (Å)	18.576(2)	19.461(4)	15.050(12)
b (Å)	12.131(4)	9.431(3)	10.504(3)
c (Å)	10.301(2)	14.306(3)	18.772(5)
β (deg)		109.78(2)	94.32(4)
V (Å^3)	2321(1)	2470(1)	2959(2)
Z	4	4	4
space group	$P2_12_12_1$	$P2_1/c$	$P2_1/n$
T (°C)	20 ± 1	20 ± 1	22 ± 1
λ (Å)	0.7093	0.7093	0.710 69
ρ_{calcd} (g cm^{-3})	1.978	1.858	2.12
μ (cm^{-1})	96.5	90.7	72.1
abs min/max	0.82/0.99	0.72/0.99	0.41/0.73
R(F)[a]	0.023	0.047	0.037
R_w(F)[b]	0.028	0.063	0.044

[a] $R(F) = \Sigma(||F_o| - |F_c||)/\Sigma(|F_o|)$. [b] $R_w(F) = [\Sigma w(|F_o| - |F_c|)^2/\Sigma w|F_o|^2]^{1/2}$ for (**1**, **2**) $w = 1/\sigma^2(F)^2 = \sigma^2$ (counts) + (pI)^2; for **4** $w = 1/(\sigma^2(F) + 0.0070F^2)$.

belong to the orthorhombic and monoclinic systems respectively while for **4** data collected on a Syntex P3 diffractometer showed that crystals belonged to the monoclinic system. The peaks of **2** were not as sharp and symmetric as usual, denoting a relatively poor quality for these crystals; a check of the unit cell using Cu Kα radiation on a Phillips PW1100/16 diffractometer gave the same results. Quantitative data were obtained at room temperature in the θ–2θ mode. The resulting data sets were transferred to a VAX computer, and for all subsequent calculations the SDP/VAX package[8] was used for **1** and **2** and SHELXTL Plus[9] was used for **4**. Three standard reflections measured every 1 h during the entire data collection periods showed no significant trends. The raw data were converted to intensities and corrected for Lorentz, polarization, and absorption effects using ψ scans of four reflections for **1** and **2** or within SHELXTL Plus for **4**, by the Gaussian method.[10] The structures were solved by the heavy-atom method. After refinement of the heavy atoms, difference-Fourier maps revealed maximas of residual electronic density close to the positions expected for hydrogen atoms. They were introduced in the structure calculations by their computed coordinates (CH = 0.95 Å) with isotropic temperature factors such as B(H) = 1.38B_{eqv}(C) Å^2 for **1** and **2** and U = 0.07 Å^2 for **4** but not refined. For **1** the absolute structure was determined by comparing $+x$, $+y$, $+z$ and $-x$, $-y$, $-z$ refinements. (R_+ = 0.023, R_{w+} = 0.0284, R_- = 0.0398, R_{w-} = 0.0513). For **4**, methyl groups were treated as rigid CH_3 units, with their initial orientation taken from the strongest H-atom peaks on a difference Fourier synthesis. Otherwise, solutions were obtained with full least-squares refinements with weighting schemes given in the table. Final difference maps revealed no significant maxima. The scattering factor coefficients and anomalous dispersion coefficients come respectively from parts a and b of ref 10. Final atom coordinates are given in Tables 3–5, and selected bond lengths and angles, in Tables 6–8.

Results and Discussion

Dihalobis(1-substituted-3,4-dimethylphosphole)platinum(II) complexes undergo a thermal dimerization of the coordinated phospholes within the coordination sphere of platinum yielding three products while photolysis of the bisphosphole starting materials gives none of these products. These products are a [4 + 2] cycloaddition product, **D**, a [2 + 2] cycloaddition product, **E**, and a third compound, **F**, in which a carbon–carbon bond is formed between carbons 2 and 2′ and a hydrogen is transferred to carbon 3 from the methyl group on carbon 3′, which is referred to as the *exo*-methylene product (see Scheme 2). Continued heating eventually converts the [4 + 2] and the [2 + 2] products into the *exo*-methylene product. This is in contrast to the thermal dimerization observed on nickel in which the major product is a diphospholene, (reaction I),[11] and the photodimerization that

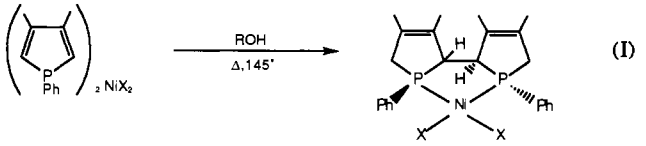

(I)

occurs on Cr, Mo and W where [2 + 2] dimers are initially

Table 3. Atom Coordinates and Equivalent Isotropic Displacement Parameters for **1**[a]

atom	x	y	z	B (Å^2)
Pt	0.07079(2)	0.17904(3)	0.12920(3)	2.759(5)
Br1	–0.01462(8)	0.0978(1)	–0.0303(1)	5.47(3)
Br2	0.16893(8)	0.1160(1)	–0.0178(1)	5.73(3)
P1	–0.0170(1)	0.2177(2)	0.2707(2)	2.61(5)
P2	0.1468(1)	0.2417(2)	0.2816(2)	2.53(5)
C1	–0.0304(5)	0.1030(7)	0.378(1)	3.0(2)
C2	–0.0134(5)	0.1241(8)	0.500(1)	3.2(2)
C3	0.0165(5)	0.2394(8)	0.5300(9)	2.9(2)
C4	0.0160(5)	0.3071(8)	0.4027(8)	2.9(2)
C5	–0.0233(6)	0.039(1)	0.607(1)	4.9(3)
C6	–0.0255(7)	0.2897(9)	0.644(1)	5.1(3)
C7	0.0982(5)	0.3171(8)	0.4079(7)	2.5(2)
C8	0.1018(5)	0.2515(8)	0.5360(8)	2.6(2)
C9	0.1466(5)	0.1488(7)	0.5117(9)	2.9(2)
C10	0.1732(5)	0.1351(7)	0.3947(8)	2.4(2)
C11	0.1312(7)	0.318(1)	0.653(1)	5.2(3)
C12	0.1615(6)	0.0694(8)	0.621(1)	3.8(2)
C13	–0.1080(6)	0.2699(9)	0.222(1)	4.1(2)
C14	–0.0983(6)	0.353(1)	0.112(1)	5.7(3)
C15	–0.1559(6)	0.175(1)	0.179(1)	6.0(3)
C16	–0.1431(6)	0.327(1)	0.339(2)	7.4(4)
C17	0.2297(5)	0.322(1)	0.236(1)	3.7(2)
C18	0.2123(6)	0.3973(9)	0.124(1)	4.8(2)
C19	0.2899(6)	0.237(1)	0.198(1)	5.0(3)
C20	0.2548(5)	0.386(1)	0.354(1)	5.0(3)

[a] Anisotropically refined atoms are given in the form of the isotropic equivalent displacement parameter defined as (4/3) [$a^2\beta(1,1) + b^2\beta(2,2) + c^2\beta(3,3) + ab(\cos\gamma)\beta(1,2) + ac(\cos\beta)\beta(1,3) + bc(\cos\alpha)\beta(2,3)$].

Table 4. Atom Coordinates and Equivalent Isotropic Displacement Parameters for **2**[a]

atom	x	y	z	B (Å^2)
Pt	0.24517(3)	0.11889(4)	0.07012(3)	4.90(1)
Br1	0.16387(9)	0.0457(1)	0.163(1)	7.73(4)
Br2	0.3370(1)	–0.0567(2)	0.1679(1)	10.55(5)
P1	0.3219(2)	0.2112(3)	0.0025(2)	5.03(7)
P2	0.1674(2)	0.2867(3)	–0.0094(2)	4.72(7)
C1	0.2908(6)	0.388(1)	–0.0534(8)	5.2(3)
C2	0.3446(7)	0.494(2)	0.003(2)	11.06(6)
C3	0.4033(6)	0.424(2)	0.085(1)	9.0(4)
C4	0.3997(7)	0.281(2)	0.096(1)	7.5(4)
C5	0.368(1)	0.608(2)	–0.041(2)	15.6(7)
C6	0.4646(9)	0.509(2)	0.166(2)	15.8(7)
C7	0.2108(6)	0.423(1)	–0.0632(9)	5.6(3)
C8	0.2011(7)	0.556(1)	–0.018(1)	9.3(4)
C9	0.1684(7)	0.539(1)	0.058(1)	6.8(4)
C10	0.1465(8)	0.414(1)	0.070(1)	7.0(4)
C11	0.163(1)	0.659(2)	0.126(2)	12.3(6)
C12	0.189(1)	0.683(2)	–0.075(2)	11.9(7)
C13	0.3525(7)	0.110(1)	–0.088(1)	7.5(4)
C14	0.4056(7)	0.197(2)	–0.123(1)	9.3(5)
C15	0.3881(8)	–0.026(2)	–0.045(2)	14.0(6)
C16	0.2873(9)	0.073(3)	–0.177(2)	18.2(7)
C17	0.0807(6)	0.234(1)	–0.1061(9)	5.8(3)
C18	0.0379(7)	0.359(2)	–0.161(1)	8.0(4)
C19	0.0311(9)	0.163(2)	–0.058(2)	12.1(6)
C20	0.0990(8)	0.143(2)	–0.182(1)	9.5(5)

[a] See footnote to Table 3.

(8) Frenz, B. A. *The Enraf-Nonius CAD4-SDP in Computing in Crystallography*; Shenk, H., Olthof-Hazekamp, H., Van Koningsveld, H., Bassi, G. C., Eds.; Delft University Press: Delft, The Netherlands, 1978; pp 64–71.
(9) Sheldrick, G. M. *SHELXTL User Manual*; Nicolet: Madison, WI, 1986.
(10) Cromer, D. T.; Waber, J. T. *International Tables for X-ray Crystallography*, Kynoch: Birmingham, England, 1974; Vol. IV: (a) Table 2.2b; (b) Table 2.3.1.
(11) Mercier, F.; Mathey, F.; Fischer, J.; Nelson, J. H. *J. Am. Chem. Soc.* **1984**, *106*, 425; *Inorg. Chem.* **1985**, *24*, 4141.

Table 5. Atom Coordinates (×10⁴) and Equivalent Isotropic Displacement Parameters (Å² × 10³) for **4**[a]

atom	x	y	z	U(eq)
Pt	1590.1(3)	1127.4(4)	1681.5(2)	31(1)
I1	3280.1(6)	607.7(9)	1465.6(5)	45(1)
I2	1191.9(6)	1441.2(10)	288.8(4)	53(1)
Cl1	7302(4)	10659(7)	1254(5)	135(3)
Cl2	7103(5)	7983(6)	1367(4)	137(3)
Cl3	5645(4)	9547(10)	851(4)	154(4)
P1	160(2)	1348(3)	1926(2)	35(1)
P2	1758(2)	815(3)	2853(2)	32(1)
C1	-557(8)	2627(12)	1613(7)	37(4)
C2	-1013(8)	2580(13)	941(7)	45(5)
C3	-1574(10)	3584(14)	720(9)	56(6)
C4	-1697(10)	4568(15)	1177(8)	57(6)
C5	-1303(11)	4642(13)	1840(8)	61(6)
C6	-702(10)	3653(13)	2057(8)	53(5)
C7	-309(8)	-198(12)	1752(6)	37(4)
C8	-206(8)	-913(13)	2320(7)	40(4)
C9	-416(11)	-2308(13)	2349(8)	59(6)
C10	134(8)	-245(11)	3034(7)	37(4)
C11	-489(10)	-639(15)	3603(8)	59(6)
C12	92(8)	1218(11)	2891(7)	38(4)
C13	953(8)	1791(11)	3310(6)	33(4)
C14	1110(9)	1251(14)	4967(7)	44(5)
C15	1130(10)	2148(12)	4684(7)	50(5)
C16	1254(9)	-21(12)	4046(6)	40(5)
C17	1470(10)	-889(15)	4647(7)	57(5)
C18	1137(9)	-501(11)	3276(6)	42(4)
C19	2842(10)	968(11)	3339(7)	42(5)
C20	3339(8)	-97(14)	3574(7)	44(5)
C21	4134(9)	81(16)	3969(7)	57(6)
C22	4431(10)	1286(14)	4170(8)	53(5)
C23	3939(9)	2348(13)	3973(7)	49(5)
C24	3128(9)	2183(13)	3539(7)	45(5)
C25	6775(11)	9344(19)	848(11)	86(8)

[a] Equivalent isotropic U defined as one-third of the trace of the orthogonalized U_{ij} tensor.

Table 6. Selected Bond Lengths (Å) and Angles (deg) for **1**

Bond Lengths			
Pt–Br1	2.488(1)	C3–C4	1.55(1)
Pt–Br2	2.491(1)	C3–C8	1.59(2)
Pt–P1	2.237(8)	C4–C7	1.53(1)
Pt–P2	2.244(3)	C7–C8	1.54(1)
C1–C2	1.32(2)	C8–C9	1.52(1)
C2–C3	1.53(2)	C9–C10	1.31(1)
Bond Angles			
Br1–Pt–Br2	86.76(5)	P1–C4–C3	108.3(7)
Br1–Pt–P1	92.78(8)	P1–C4–C7	113.8(7)
Br2–Pt–P2	93.94(8)	C3–C4–C7	90.3(8)
P1–Pt–P2	86.1(1)	P2–C7–C4	115.3(7)
C1–P1–C4	92.7(5)	P2–C7–C8	109.2(7)
C7–P2–C10	91.9(5)	C4–C7–C8	91.8(7)
P1–C1–C2	113.8(8)	C3–C8–C7	88.4(8)
C1–C2–C3	117(1)	C3–C8–C9	117.5(9)
C2–C3–C4	108.2(9)	C8–C9–C10	117.4(9)
C2–C3–C8	116.9(9)	C7–C8–C9	107.8(9)
C4–C3–C8	89.4(8)	P2–C10–C9	113.5(8)

formed but they subsequently undergo thermal rearrangements to the [4 + 2] products.[12]

X-ray crystal structures were obtained for an example of each of the three types of compounds: **1**, the [2 + 2] cycloaddition product (Figure 1), **2**, the exomethylene product (Figure 2) from thermolysis of *cis*-dibromobis(1-*tert*-butyl-3,4-dimethylphosphole)platinum(II), and **4** (Figure 3), a [4 + 2] cycloaddition product from the reaction of *cis*-$(DMPP)_2PtCl_2$ with *cis*-$(DMPP)_2PtI_2$. See Tables 6–8 for relevant bond distances and bond angles. Each of the compounds crystallizes as discrete molecular entities with no unusual intermolecular contacts. The coordination geometry about platinum in each compound is

(12) Santini, C. C.; Fischer, J.; Mathey, F.; Mitschler, A. *J. Am. Chem. Soc.* **1980**, *102*, 5809.

Table 7. Selected Bond Lengths (Å) and Angles (deg) for **2**

Bond Lengths			
Pt–Br1	2.484(1)	C1–C7	1.55(2)
Pt–Br2	2.491(2)	C2–C3	1.49(2)
Pt–P1	2.214(3)	C2–C5	1.40(2)
Pt–P2	2.219(3)	C3–C4	1.36(2)
P1–C1	1.86(1)	C7–C8	1.46(2)
P1–C4	1.77(1)	C8–C9	1.43(2)
P2–C7	1.84(1)	C8–C12	1.42(2)
P2–C10	1.79(1)	C9–C10	1.29(2)
C1–C2	1.48(2)		
Bond Angles			
Br1–Pt–Br2	88.90(6)	C3–C2–C5	114(1)
Br1–Pt2–P2	91.42(8)	C2–C3–C4	118(1)
Br2–Pt–P1	92.58(8)	P1–C4–C3	110(1)
P1–Pt–P2	86.5(1)	P2–C7–C1	113.8(7)
C1–P1–C4	93.5(7)	P2–C7–C8	105.5(8)
C7–P2–C10	92.0(6)	C1–C7–C8	114.8(9)
P1–C1–C2	107.7(9)	C7–C8–C9	113(1)
P1–C1–C7	113.5(6)	C7–C8–C12	119(2)
C2–C1–C7	114(1)	C9–C8–C12	120(1)
C1–C2–C3	110(1)	C8–C9–C10	117(1)
C1–C2–C5	123(2)	P2–C10–C9	112(1)

Table 8. Selected Bond Lengths (Å) and Angles (deg) for **4**

Bond Lengths			
Pt–I1	2.662(2)	C7–C8	1.304(17)
Pt–I2	2.658(2)	C8–C10	1.564(18)
Pt–P1	2.247(3)	C10–C12	1.560(16)
Pt–P2	2.219(3)	C10–C18	1.567(18)
P1–C7	1.791(12)	C12–C13	1.583(16)
P1–C12	1.826(13)	C13–C14	1.531(17)
P2–C13	1.848(12)	C14–C16	1.354(18)
P2–C18	1.878(11)	C16–C18	1.529(17)
Bond Angles			
I2–Pt–I1	91.3(1)	C10–C12–P1	103.9(8)
P1–Pt–I2	92.3(1)	C13–C12–P1	111.1(8)
P2–Pt–I1	94.7(1)	C13–C12–C10	105.6(10)
P2–Pt–P1	81.5(1)	C12–C13–P2	95.6(7)
C12–P1–C7	93.6(5)	C14–C13–P2	99.5(8)
C18–P2–C13	81.2(5)	C14–C13–C12	112.6(10)
C8–C7–P1	110.6(9)	C16–C14–C13	110.6(11)
C10–C8–C7	116.9(11)	C18–C16–C14	110.2(10)
C12–C10–C8	106.8(10)	C10–C18–P2	104.5(7)
C18–C10–C8	114.6(10)	C16–C18–P2	97.5(8)
C18–C10–C12	104.1(10)	C16–C18–C10	104.9(10)

Scheme 2

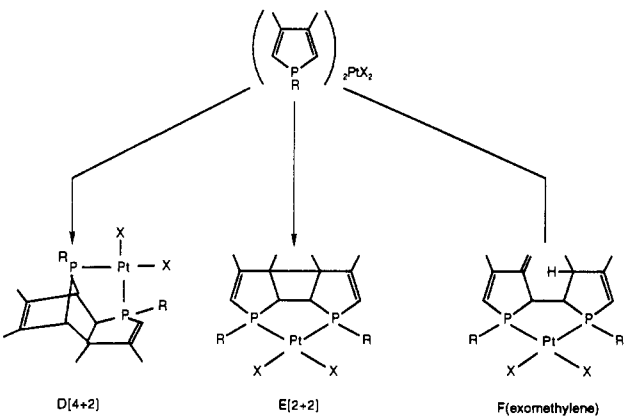

essentially planar as the sums of the bond angles around platinum are very near 360°. The Pt–P bond distances are slightly different in **1** (2.237(3), 2.244(3) Å), equal in **2** (2.214(3), 2.219(3) Å), and considerably different in **4** (2.219(3), 2.247(3) Å). Of particular note are the relatively long C3–C8 (1.59(2) Å), **1**, and C12–C13 (1.583(16) Å) and C10–C18 (1.567(18) Å) bond distances for **4**. These are the bonds that are cleaved in the thermal conversion of the [2 + 2] and [4 + 2] compounds to the *exo*-methylene compound. It is also important to note that for each of these compounds the bond formation between what was

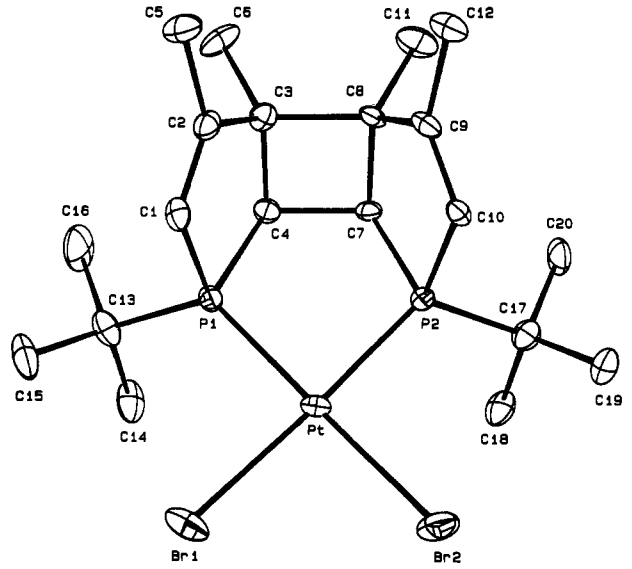

Figure 1. ORTEP drawing of 1 showing the atom-numbering scheme. (50% probability ellipsoids). Hydrogen atoms are omitted.

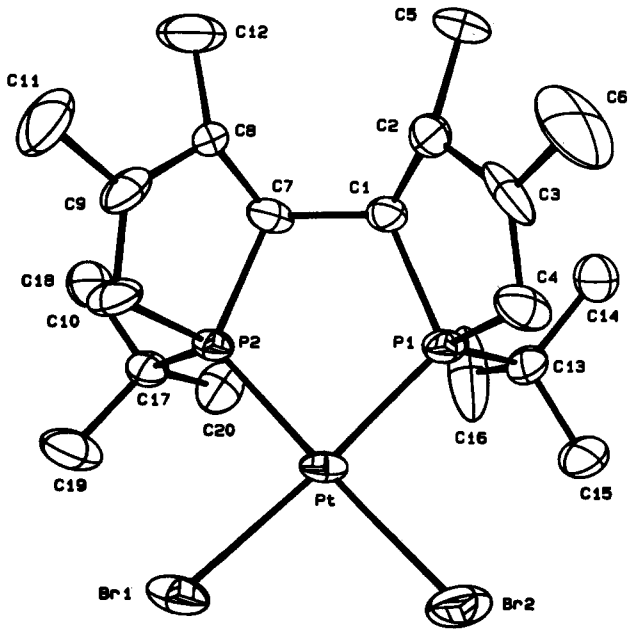

Figure 2. ORTEP drawing of 2 showing the atom-numbering scheme. (50% probability ellipsoids). Hydrogen atoms are omitted.

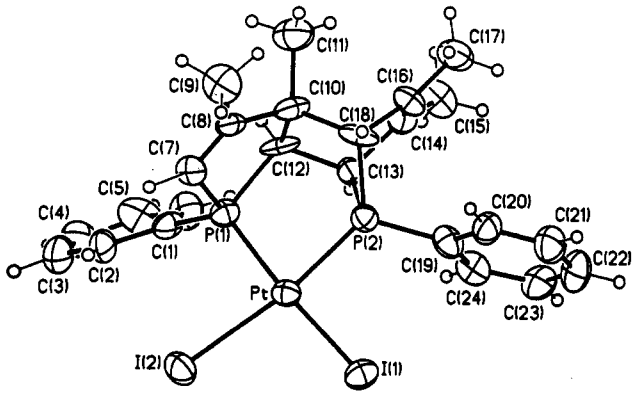

Figure 3. View of 4 showing the atom numbering scheme (50% probability ellipsoids). Hydrogen atoms have an arbitrary radius of 0.1 Å.

originally carbons 2 and 2′ in the complexes occurred syn with respect to the original phosphole rings. In *cis*-dichlorobis(1-phenyl-3,4-dimethylphosphole)platinum(II), $(DMPP)_2PtCl_2$, the distance between C(124) and C(224) (4.84 (Å))[13] shortens to 1.53(1) Å (C4C7) in **1**, 1.55(2) Å (C1C7) in **2**, and 1.583(16) Å (C12C13) in **4**, demonstrating the considerable molecular motion occurring during the course of the solid-state reactions. From the crystal structure of **2**, becuase of the poor crystal quality, it is impossible to determine whether carbon 5 or carbon 12 is the exomethylene carbon. The C1C2C3 and C7C8C12 bond angles are both indicative of sp^2 hybridization. The C2C5 and C8C12 bond distances of 1.40 and 1.42 Å respectively are intermediate between the single bond length of 1.47 Å (from the average of the C1C2 and C7C8 distances) and the double bond length of 1.37 Å (from the average of the C3C4 and C9C10 bond distances). Also, in the presence of the heavy Pt and Br atoms the accuracy of the C–C bond lengths and CCC bond angles is relatively poor. Fortunately, the structure of this compound could be completely confirmed from NMR data.

To confirm the structure of **2**, ^1H, $^{13}C\{^1H\}$, $^{31}P\{^1H\}$, broad-band $^1H\{^{31}P\}$, selective $^1H\{^{31}P\}$, ^1H COSY, $^1H/^{13}C$ HETCOR, and ^{13}C APT NMR spectra were obtained. The ^{31}P NMR spectrum of **2** contained two doublets of equal intensity at δ 102.6 (P_1) and 87.2 ppm (P_2) with ^{195}Pt satellites and a $^2J(PP)$ coupling constant of 3.0 Hz. The $^1J(PtP)$ coupling constants were 3286 and 3518 Hz, respectively. These data are indicative of a *cis*-P_2PtBr_2 compound.[6,13] The ^1H NMR spectrum (see structure **2** for proton labeling)consisted of two doublets of quartets inte-

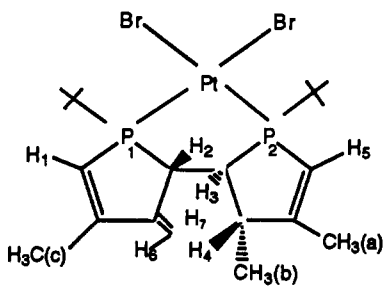

2

grating for one proton each at δ 6.48 (H_1) and δ 6.14 ppm (H_5) for which the $^2J(PH)$ coupling constants of 26.4 and 27.9 Hz, respectively, the $^3J(PH)$ coupling constants of 22.5 Hz each and the $^4J(HH)$ couplings of 1.0 and 1.5 Hz, respectively, are indicative of protons on vinyl carbons α to a phosphorus and allylic to a methyl group; two singlets at δ 5.63 (H_6 or H_7) and δ 5.46 ppm (H_7 or H_6) integrating for one proton each; a one proton doublet of doublets at δ 3.37 ppm ($^2J(P_1H)$ = 3.5 Hz, $^2J(H_2H_3)$ = 10.5 Hz) H_2; a one proton multiplet at δ 2.52 ppm (dddd, $^3J(P_1H)$ = 32.1 Hz, $^3J(H_2H_3)$ = 10.5 Hz, $^2J(P_2H)$ = 9.0 Hz, $^3J(H_3H_4)$ = 6.9 Hz) H_3; a three proton apparent triplet at δ 2.07 ppm ($^4J(H_1$-$CH_3)$ = $^4J(P_1CH_3)$ = 1.5 Hz, $^5J(PtH)$ = 3.0 Hz), CH_3(c); a one proton multiplet at δ 1.81 ppm, H_4, obscured by an apparent doublet of triplets at δ 1.79 ppm ($^4J(P_2CH_3)$ = 2.1 Hz, $^4J(H_5$-$CH_3)$ = $^4J(H_4CH_3)$ = 1.0 Hz, $^4J(PtH)$ = 12 Hz) CH_3(a); two doublets at δ 1.34 ($^3J(P_2H)$ = 16.2 Hz) and δ 1.29 ($^3J(P_1H)$ = 15.6 Hz) representing nine protons each (two *tert*-butyl groups); and a three proton doublet at δ 1.19 ($^3J(H_4CH_3)$ = 7.0 Hz, CH_3-(b)). The PH couplings were affirmed by $^1H\{^{31}P\}$ decoupling experiments. The $^{13}C\{^1H\}$ NMR spectrum combined with the $^{13}C\{^1H\}$ APT spectrum (Figure 4) showed there to be 16 chemical shift inequivalent carbons. There are methyl group resonances at δ 16.44 (d, $^3J(PC)$ = 12.5 Hz, $^4J(PtC)$ = 19.0 Hz, CH_3(c)), 19.38 (d, $^3J(PC)$ = 14.7 Hz, $^4J(PtC)$ = 19.0 Hz, CH_3(a)), 22.33 (d, $^3J(PC)$ = 3.2 Hz, $^4J(PtC)$ = 20.7 Hz, CH_3(b)), 28.01 (d, $^2J(PC)$ = 2.9 Hz, $^3J(PtC)$ = 11.6 Hz), and 28.33 (d, $^2J(PC)$ = 3.2 Hz, $^3J(PtC)$ = 11.6 Hz). The latter two resonances are assigned to the methyls of the *tert*-butyl groups. The two *tert*-butyl quaternary carbon resonances occur at δ 33.80 (d, $^1J(PC)$

(13) Holt, M. S.; Nelson, J. H.; Alcock, N. W. *Inorg. Chem.* **1986**, *25*, 2288.

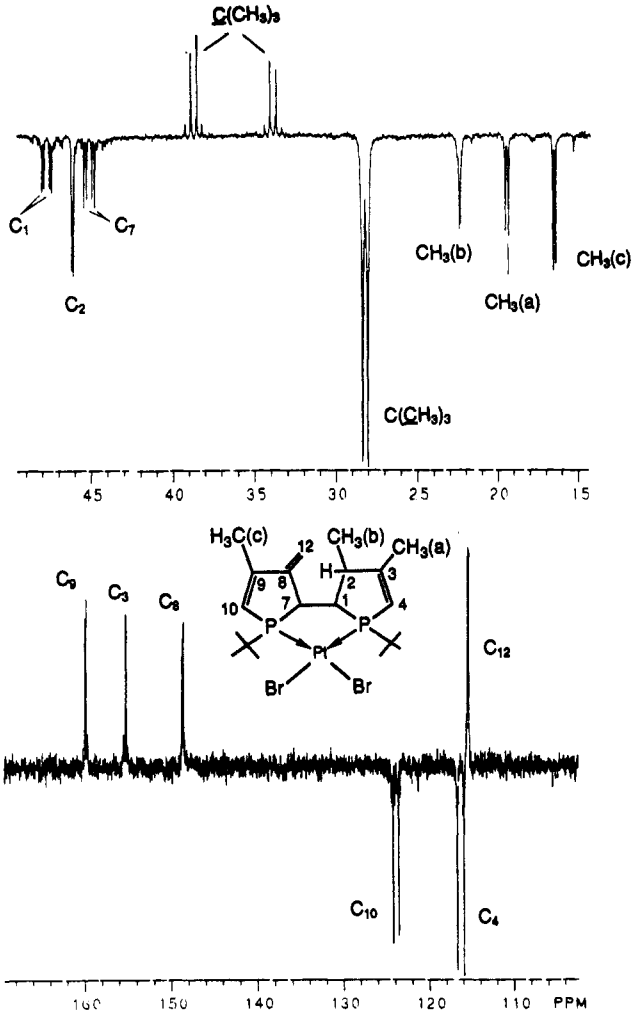

Figure 4. 75 MHz $^{13}C\{^1H\}$ APT spectrum of **2** in $CDCl_3$: C, CH_2 (up); CH, CH_3 (down).

= 28.6 Hz, ^2J(PtC) = 49.0 Hz) and 38.64 (d, ^1J(PC) = 28.9 Hz, ^2J(PtC) = 48.7 Hz). There are three methine carbon resonances at δ 45.10 (dd, ^1J(PC) = 37.3 Hz, ^2J(PC) = 13.0 Hz, ^2J(PtC) = 100.1 Hz, C_7), 46.11 (d, ^2J(PC) = 7.1 Hz, C_2), and 47.74 (dd, ^1J(PC) = 35.1 Hz, ^2J(PC) = 9.7 Hz, ^2J(PtC) = 102.6 Hz, C_1). There is one vinyl carbon (=CH_2) resonance at δ 115.33 (d, ^3J(PC) = 8.4 Hz, ^4J(PtC) = 15.3 Hz, C_{12}). There are two vinyl carbon (=CH) resonances at δ 116.27 (d, ^1J(PC) = 59.3 Hz, ^2J(PtC) = 13.8 Hz, C_4) and 123.81 (d, ^1J(PC) = 48.8 Hz, ^2J(PtC) = 28.6 Hz, C_{10}). The coupling constants are indicative of carbons directly bonded to phosphorus. There are three vinyl carbon resonances representing carbons with no attached protons at δ 148.58 (dd, ^2J(PC) = 9.6 Hz, ^3J(PC) = 7.5 Hz, ^3J(PtC) = 22.4 Hz, C_8), 155.13 (d, ^2J(PC) = 5.1 Hz, ^3J(PtC) = 37.0 Hz, C_3), and 159.80 (d, ^2J(PC) = 11.3 Hz, ^3J(PtC) = 32.6 Hz, C_9). Where applicable, the assignments were affirmed by a $^1H/^{13}C$ HETCOR spectrum. The NMR spectral data together with the crystal structures show that the products of the thermolyses reactions are as shown in Scheme 2.

Kinetics

Comparative Rates. Various (1-substituted-3,4-dimethylphosphole)$_2PtX_2$ complexes were heated at reflux (145 °C) in 1,1,2,2-tetrachloroethane for 18 h to ascertain the effects of the phosphorus substituent and X on the product distribution and relative rates of reaction (Table 1). The products of these thermolyses were determined by $^{31}P\{^1H\}$ NMR spectra (Table 9) of the reaction mixtures and except as described above were not isolated. It was observed that the (phosphole)$_2PtX_2$ complexes that possess a cis geometry in this solvent at this temperature were completely converted to the products illustrated in scheme 2. In contrast, diiodobis(1-phenyl-3,4-dimethylphosphole)platinum(II) and diiodobis(1-benzyl-3,4-dimethylphosphole)platinum(II), both of which are wholly trans under these conditions, were recovered unchanged. This suggests that the phosphole dimerizations occur intramolecularly. In comparison, analogous thermolyses of $(DMPP)_2PdCl_2$ produce an additional product (G) by an intermolecularcoupling of two phospholes followed

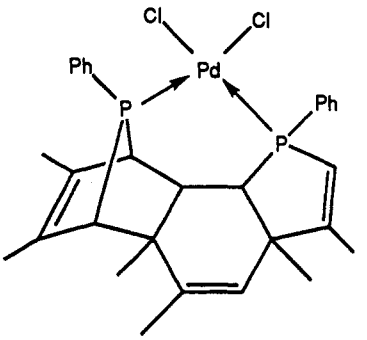

G

sequentially by phosphinidene elimination and [4 + 2] cycloaddition.[3] The chloride and bromide complexes of the *tert*-butylphosphole reacted at similar rates. For the chloride and bromide complexes, the bulkier the phosphorus substituent, the faster the reaction. Also, the amount of the [4 + 2] product generally decreases and the amount of the [2 + 2] product generally increases with increasing steric bulk of the phosphorus substituent.

Detailed Kinetics. Detailed kinetic runs were performed on $(DMPP)_2PtCl_2$ in 1,1,2,2-tetrachloroethane solution at 145 °C and in the solid-state at 140 °C. Above 215 °C and solid melts[6] and polymerization occurs. The results of the solution and solid-state studies are shown in Figures 5–7, respectively. The loss of the starting material is clearly first order (Figure 5), implying a unimolecular mechanism. A proposed mechanism is shown in Scheme 3. Though the [2 + 2], [4 + 2] and exomethylene products could also be formed by independent electrocyclic and ene reactions, we favor the mechanism shown in Scheme 3 for its simplicity. The starting material (**H**) reacts by forming a bond between carbon 2 and carbon 2′ of two adjacent phospholes to generate a diallyl 1,4-biradical intermediate (**I**). This intermediate, which is never observed, then collapses by additional carbon–carbon bond formation or [1,5]-hydrogen migration to the observed [2 + 2] (**J**), [4 + 2] (**K**), and *exo*-methylene products (**L**). As can be seen in Figures 6 and 7 the [2 + 2] and [4 + 2] products are in equilibrium with the intermediate while the exomethylene product is formed irreversibly. The reaction is thus ultimately driven to the exomethylene product. (See previous discussion of C–C bond distances). This mechanism gives rise to the following rate laws, eqs 1–5. According to this mechanism,

$$\frac{d[\mathbf{H}]}{dt} = -k_1[\mathbf{H}] \quad (1)$$

$$\frac{d[\mathbf{I}]}{dt} = k_1[\mathbf{H}] + k_2[\mathbf{K}] + k_3[\mathbf{J}] - (k_2 + k_3 + k_4)[\mathbf{I}] \quad (2)$$

$$\frac{d[\mathbf{L}]}{dt} = k_4[\mathbf{I}] \quad (3)$$

$$\frac{d[\mathbf{K}]}{dt} = k_2[\mathbf{I}] - k_{-2}[\mathbf{K}] \quad (4)$$

$$\frac{d[\mathbf{J}]}{dt} = k_3[\mathbf{I}] - k_{-3}[\mathbf{J}] \quad (5)$$

Table 9. 121.65-MHz $^{31}P\{^1H\}$ NMR Data for the Products of Thermolysis of (1-Substituted-3,4-dimethylphosphole)$_2$PtX$_2$ Complexes in $CDCl_3$ at 300 K, (δ (ppm); J (Hz))

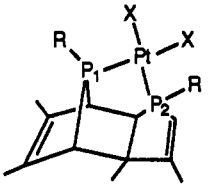

[4 + 2]

X	R	$\delta(P_1)$	$\delta(P_2)$	^2J(P–P)	$^1J(P_1$–Pt)	$^2J(P_2$–Pt)
Br	*n*-butyl	105.2	42.2	12	3241	2985
Cl	methyl	94.5	31.1	17	3298	3120
Cl	phenyl	109.2	40.5	15	3252	3187
Br	benzyl	107.3	44.2	12	3228	3032

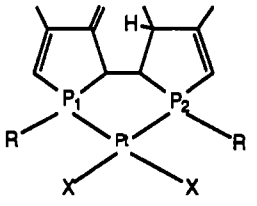

(*exo*-methylene)

X	R	$\delta(P_1)$	$\delta(P_2)$	^2J(P–P)	$^1J(P_1$–Pt)	$^1J(P_2$–Pt)
Br	*tert*-butyl	102.6	87.2	3.0	3286	3518
Cl	*tert*-butyl	96.8	76.3	5.8	3594	3569
Br	*n*-butyl	86.8	75.4	3.5	3274	3562
Cl	phenyl	81.8	70.0	0.0	3447	3687
Br	benzyl	83.1	74.7	7.0	3462	3501

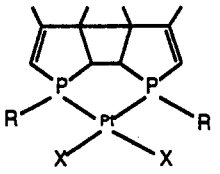

[2 + 2]

X	R	δP	^1J(P–Pt)
Br	*tert*-butyl	97.2	3538
Cl	*tert*-butyl	92.1	3562
Br	*n*-butyl	81.9	3513
Cl	methyl	69.8	2916
Br	benzyl	80.3	3535
Cl	phenyl	80.5	3650

the loss of starting material is independent of any other compounds, therefore an approximate value of $k_1 = (5.8 \pm 0.3) \times 10^{-5}$ s^{-1} is determined directly. Approximate values of k_2, k_3, and k_4 were determined from the initial rates of formation of **K**, **J**, and **L** respectively. Approximate values of k_{-2} and k_{-3} were obtained from the rates of disappearance of **K** and **J** respectively. Then eqs 1–5 were integrated numerically to find the temporal behavior of the concentration of each species. Since the intermediate, **I**, is not observable experimentally, the calculated percent composition of the reaction mixture was based only on the relative amounts of **H**, **J**, **K**, and **L** (that is, **H** + **J** + **K** + **L** = 100%). The rate constants were then adjusted to give the fit to the experimental data.

The validity of this mechanism is shown in the concentration *vs* time graphs of the various components (Figures 6 and 7). Since, the rate of formation of the [4 + 2] cycloaddition product from the intermediate is 3.4 times the rate of formation of the [2 + 2] cycloaddition product ($k_2/k_3 = 3.39$), its concentration is initially expected to increase more rapidly. But since its decomposition is about 9 times as rapid ($k_{-2}/k_{-3} = 8.75$), its concentration is expected to peak earlier. Indeed, the concentration of the [2 + 2] product is still increasing while the

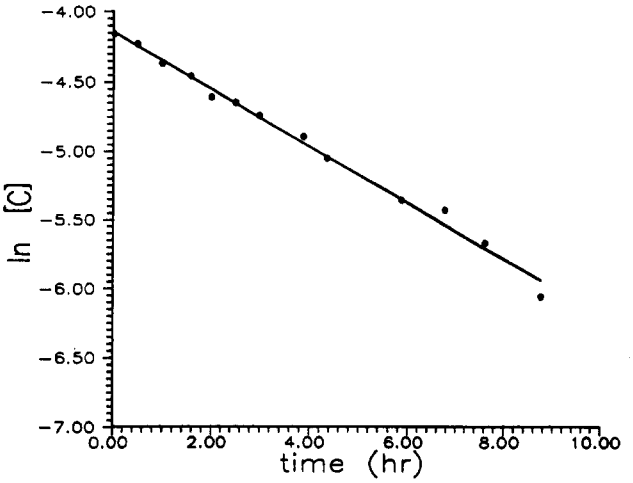

Figure 5. First-order plot for the disappearance of $(DMPP)_2PtCl_2$ in $Cl_2CHCHCl_2$ at 145 °C. The apparent value of k_1 is $(5.8 \pm 0.3) \times 10^{-5}$ s^{-1}.

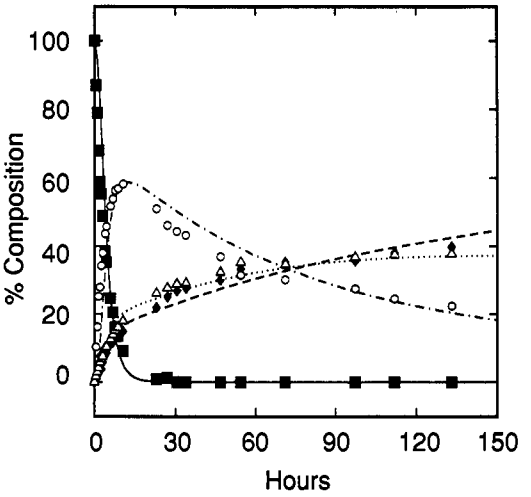

Figure 6. Percent composition as a function of time for the thermolysis of $(DMPP)_2PtCl_2$ in $Cl_2CHCHCl_2$ at 145 °C: (■) starting material experimental; (—) starting material calculated; (○) [4 + 2] experimental; (– • –) [4 + 2] calculated; (△) [2 + 2] experimental; (···) [2 + 2] calculated; (◇) [exo] experimental; (- - -) [exo] calculated. The lines were calculated from the following rate constants: $k_1 = (8.33 \pm 0.3) \times 10^{-5}$ s^{-1}, $k_2 = (5.28 \pm 0.3) \times 10^{-5}$ s^{-1}; $k_3 = (1.56 \pm 0.3) \times 10^{-5}$ s^{-1}; $k_4 = (1.25 \pm 0.3) \times 10^{-5}$ s^{-1}; $k_{-2} = (9.72 \pm 0.3) \times 10^{-6}$ s^{-1}; $k_{-3} = (1.11 \pm 0.3) \times 10^{-6}$ s^{-1}.

concentration of the [4 + 2] compound rapidly decreases (note the relative slopes in Figure 6). It is also important to note that while the rate of formation of the [2 + 2] cycloaddition product from the intermediate is 1.2 times the rate of formation of the exomethylene product, the [2 + 2] cycloaddition product is in equilibrium with the intermediate. As a consequence, the concentrations of the [2 + 2] cycloaddition and exomethylene products remain roughly equal in the early stages of the reaction. Eventually, the irreversibility of the formation of the *exo*-methylene product starts to become apparent and their concentrations differ.

The same mechanism apparently holds for the solid-state reaction but with differences in the various rate constants; e.g., $k_1 = (6.1 \pm 0.3) \times 10^{-5}$ s^{-1} for $(DMPP)_2PtCl_2$. The rate of formation of the intermediate from the starting material is slightly less than in solution. The solid-state reactions are topotactic;[14] the products are formed in the crystal lattice of the reactant. The fact that the solid-state reactions proceed slightly more slowly than those in solution is most likely due to the fact that the required

(14) Desiraju, G. R. *Proc. Indian Nat. Sci. Acad., Part A* **1986**, *52*, 379.

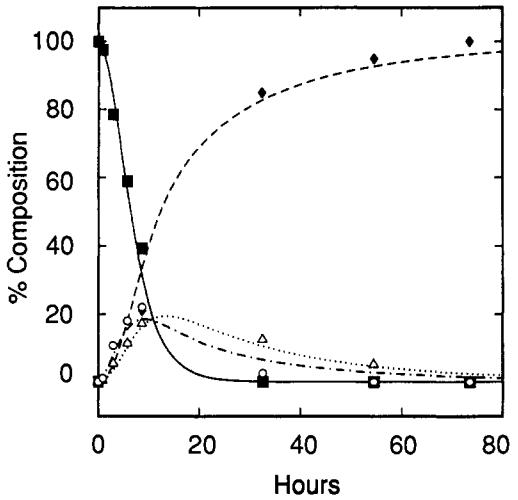

Figure 7. Percent composition as a function of time for the thermolysis of $(DMPP)_2PtCl_2$ in the solid state at 140 °C. The symbols are the same as in Figure 6. $k_1 = (6.11 \pm 0.3) \times 10^{-5}$ s^{-1}; $k_2 = (5.0 \pm 0.3) \times 10^{-5}$ s^{-1}; $k_3 = (1.0 \pm 0.3) \times 10^{-5}$ s^{-1}; $k_4 = (1.25 \pm 0.3) \times 10^{-5}$ s^{-1}; $k_{-2} = (3.06 \pm 0.3) \times 10^{-4}$ s^{-1}; $k_{-3} = (4.44 \pm 0.3) \times 10^{-5}$ s^{-1}.

Scheme 3

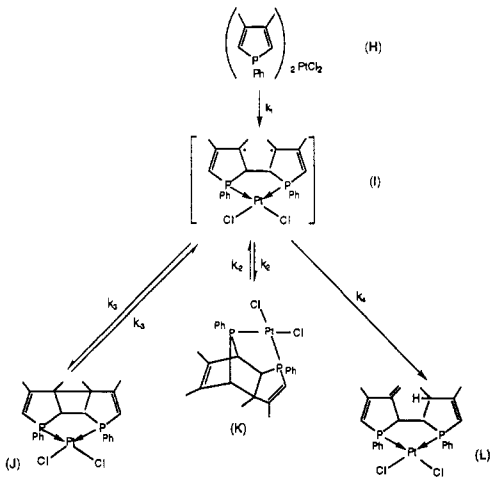

relative positions of the phosphole rings is more difficult to attain in the solid state due to restricted rotational motion. The subsequent reactions of the [4 + 2] and the [2 + 2] cycloaddition products are considerably more rapid in the solid state, and their relative decomposition rates are the same in the solid state as in solution (compare Figures 6 and 7). In the solid state, any thermal energy that is added to the system has to go into librational or vibrational modes as translational modes are extremely unlikely below the melting point. Thus, at a given temperature, it is easier to break bonds in the solid state than in solution, and the concentration of the intermediate should thusly be larger. Increasing the concentration of the intermediate should increase the rate of formation of the exomethylene product. Indeed, at 70 h in the solid state the reaction has gone to completion, while after 70 h in solution the *exo*-methylene product represents only 35% of all species in solution.

Conclusions

The thermolyses of dihalobis(1-R-3,4-dimethylphosphole)-platinum(II) complexes most likely proceed via a branching mechanism with ultimate formation of the exomethylene products. The branches evolve from the common intermediate, 1,4-butanediyl biradical.[15] In both the solution and solid states, the reaction proceeds only if the starting complex has the cis geometry; the trans geometry precludes intramolecular carbon–carbon bond formation. The nature of the halide affects the reaction only in the determination of the geometry of the complexes. The larger the halide the more thermodynamically stable the trans isomer. There are minimal differences in the reaction rates and product distributions between the chloride and bromide complexes, and no reaction occurs for the iodide complexes which have the trans geometry. The phosphorus substituent affects the reaction by altering the relative stabilities of the various products. This appears not to be electronic in nature, but rather a function of steric bulk. Bulky substituents decrease the stability of the [4 + 2] cycloaddition product while small substituents likely methyl or sterically flexible substituents like benzyl increase the relative stability of the [4 + 2] cycloaddition product. A few comments are in order with regard to the function of the metal.

Thermolyses of phospholes, their oxides and sulfides, in the absence of a transition metal take entirely different courses as illustrated in reactions II–IV.

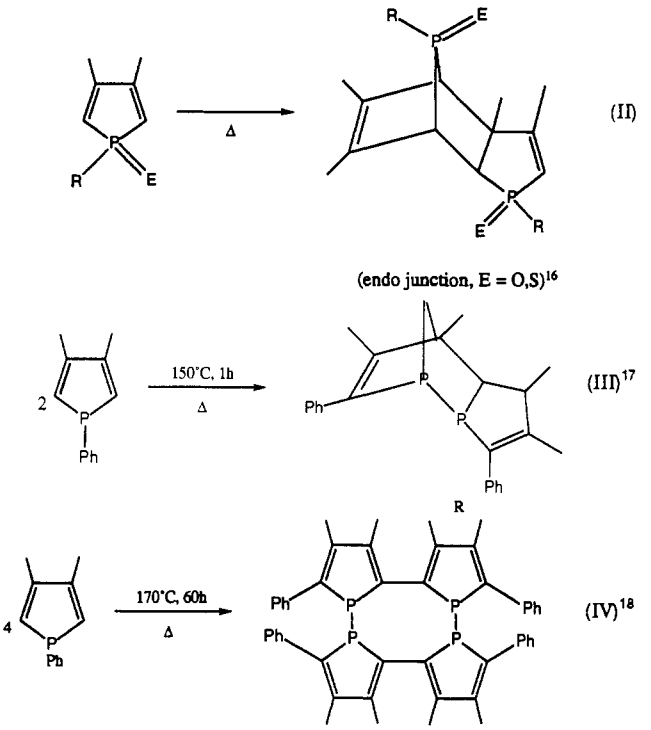

No products of these types, especially the end [4 + 2] dimer such as illustrate in reaction II, were observed in the thermolyses of the $(phosphole)_2PtX_2$ complexes. The endo [4 + 2] dimer is thermodynamically more stable than the exo [4 + 2] dimer. Lack of formation of these products supports our contention of the intramolecular nature of the thermolyses of $(phosphole)_2PtX_2$. Further, phosphole dissociation would cause associative phosphole ligand exchange by forming pentacoordinate $(phosphole)_3PtX_2$ complexes in solution.[19] Crossover experiments to test the intramolecular nature of these reactions are not possible because of the ligand redistribution reactions illustrated in Scheme 1. Thermolyses of the nickel complexes probably occur by a similar mechanism but at a tetrahedral metal center and then the phosphole dimerization is anti and is followed by intermolecular

(15) For recent discussions of biradical intermediates, see: Peterson, T. H.; Carpenter, B. K. *J. Am. Chem. Soc.* **1992**, *114*, 1496. Ariel, S.; Evans, S. V.; Garcia-Garibsay, M.; Harkness, B. R.; Omkaram, N.; Scheffer, J. R.; Trotter, J. *J. Am. Chem. Soc.* **1988**, *110*, 5591.
(16) Mathey, F.; Mankowski-Favelier, R. *Bull. Soc. Chim. Fr.* **1970**, 4433.
(17) Mercier, F.; Mathey, F. *J. Organomet. Chem.* **1984**, *263*, 55.
(18) Mathey, F.; Mercier, F.; Nief, F.; Fischer, J.; Mitschler, A. *J. Am. Chem. Soc.* **1982**, *104*, 2077.
(19) MacDougall, J. J.; Nelson, J. H.; Mathey, F. *Inorg. Chem.* **1982**, *21*, 2145.

hydrogen abstraction to give the diphospholene.[11] On chromium, molybdenum or tungsten the [2 + 2] dimer rearranges at ambient temperature to the [4 + 2] dimer.[12] The $[(\eta^5\text{-}C_5H_5)Ru\text{-}(DMPP)_2L]PF_6$ complexes undergo sunlight-initiated [2 + 2] phosphole dimerizations,[20] and these compounds do not rearrange below their decomposition points. The influence of the metal on the relative thermodynamic stabilities of the various phosphole dimers may be related to the bite angle in the chelate ring. A reduction in the PMP angle would induce increasing strain on the C3–C8 bond of the [2 + 2] dimer and on the C10–C18 and C12–C13 bonds of the [4 + 2] dimer. Further studies are in progress to gain more information on this point.

Acknowledgment. We are grateful to the donors of the Petroleum Research Fund, administered by the American Chemical Society, for financial support and to Johnson Mathey Aesar/Alfa for their generous loan of potassium tetrachloroplatinate(II).

Supplementary Material Available: For the crystal structures, listings of crystal and refinement data, bond distances and angles, H atom coordinates, and thermal parameters (17 pages). Ordering information is given on any current masthead page.

(20) Ji, H.-L.; Ph.D. Dissertation, University of Nevada, Reno, 1991.